

Millimeter and Submillimeter Wave Spectrum of $^{18}\text{O}_2$ †

Wayne Steinbach and Walter Gordy

Department of Physics, Duke University, Durham, North Carolina 27706

(Received 30 May 1973)

Fine-structure transitions in the millimeter wavelength region and the $n(J) = 1(2) - 3(2)$ submillimeter wavelength rotational transition have been measured with high precision. The submillimeter radiation was generated by a harmonic multiplier and detected by a silicon bolometer operated at 1.5 °K. The measured $1(2) - 3(2)$ frequency of $^{18}\text{O}_2$ is 378 831.51(20) MHz. A remeasurement of the $1(2) - 3(2)$ frequency for $^{16}\text{O}_2$ yielded the value 424 763.12(10) MHz. Analysis of the results yielded the following values of the molecular constants for $^{18}\text{O}_2$: $B_0 = 38\,313.721(2)$ MHz, $\lambda_0 = 59\,496.708(12)$ MHz, $\lambda_1 = 0.0521(3)$ MHz, $\mu_0 = -224.438(3)$, $\mu_1 = -0.000\,29(5)$ MHz, $B_e = 38\,518.6(6.3)$ MHz, and $r_e = 1.20\,743(10)$ Å. The values agree well with those predicted from isotopic corrections of the $^{16}\text{O}_2$ values. The equilibrium constants were obtained with the aid of vibration-rotation interaction constants from optical spectroscopy.

INTRODUCTION

Although the $^{16}\text{O}_2$ molecule has been studied extensively in the microwave region,¹⁻⁴ to the best of our knowledge no high-precision microwave measurements have been made on $^{18}\text{O}_2$. Each isotopic species has a millimeter wave spectrum arising from transitions between electronic fine-structure levels of given rotational states and a submillimeter wavelength spectrum arising from transitions between rotational states. Miller, Javan, and Townes⁵ observed four fine-structure transitions of $^{18}\text{O}_2$ between 58 300 and 59 900 MHz for the purpose of establishing the zero nuclear spin of $^{18}\text{O}_2$, but they did not report accurate line frequencies.

The rotational spectra of $^{18}\text{O}_2$ and $^{16}\text{O}_2$ are rather exceptional because alternate rotational levels are missing and because the molecules have no electric dipole moment. The nuclei of $^{18}\text{O}_2$ are identical Bose particles, and therefore the over-all wave function must be symmetric. Because the $^3\Sigma_g^-$ electronic ground state is odd, levels with even rotational quantum numbers do not occur. These features are illustrated in Fig. 1. All observable transitions in O_2 are induced by its electronic spin magnetic moment. The rotational transitions result from a coupling of this spin-dipole moment with the molecular-rotational axis. The strengths of such transitions are orders of magnitude smaller than those of similar transitions induced by a typical electric-dipole moment of 1 D. Probabilities for induced rotational transitions in O_2 have been theoretically predicted by Tinkham and Strandberg.⁶

EXPERIMENTAL PROCEDURES

Microwave radiation for observation of the submillimeter rotational transitions was produced

by a klystron-driven crystal harmonic generator, earlier developed in this laboratory.⁷ Fundamental klystron power was used in the measurement of the low-frequency (57–62-GHz) transitions. The klystron frequency was accurately measured by means of a comparison with a frequency referenced to station WWVB of the National Bureau of Standards. A tapered horn and Teflon lens were used for coupling radiation into the absorption cell which consisted of a glass tube 3 m long and 22 mm in diameter; the tube was coated on the inside with silver. A modulation coil was wrapped around the cell to provide an axial magnetic field. The entire cell was immersed in a liquid-nitrogen bath. A diagram of the spectrometer is shown in Fig. 2. The oxygen sample contained 99.40% enriched $^{18}\text{O}_2$.

Detection of the low-frequency transitions was accomplished by means of a 1N53 crystal mounted on the waveguide. Submillimeter radiation was detected with the silicon bolometer arranged as shown in Fig. 3. A commercial silicon chip obtained from the Far Infrared Division of the Molelectron Corp. was employed. It was mounted at the center of an integrating sphere. Cooled filters consisting of black polyethylene and crystalline quartz shielded the chip from room-temperature black-body radiation. The detecting element was placed in a liquid-helium bath. By pumping on the liquid helium we were able to obtain operating temperatures of 1.5 °K.

In sensitivity, this detector is comparable to the InSb detector already in use in this laboratory,⁸ but it has a slower response time. The slow response is not a hindrance, however, when the detector is used to detect modulated signals in the low audio-frequency range. Thus, we were able to use modulation frequencies as high as 450 cps without noticeable losses due to detector response.

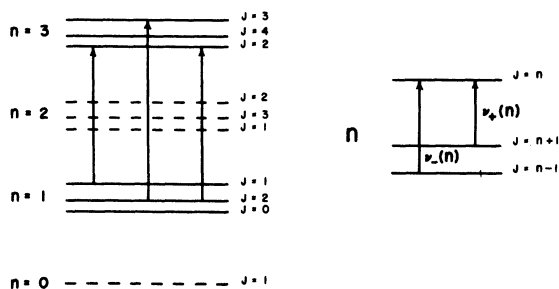


FIG. 1. Energy-level diagram for $^{18}\text{O}_2$. Dashed lines indicate forbidden levels.

Zeeman modulation¹ of the lines was used in the detection of all of the transitions. A sinusoidal magnetic field was applied to produce amplitude modulation of the radiation at the line frequencies. The modulated signal detected by the bolometer was then preamplified and fed into a phase-sensitive lock-in amplifier tuned to twice the modulation frequency. The output signal, a second-derivative line shape, was displayed on either a chart recorder or an oscilloscope trace.

To circumvent decrease in accuracy due to broadening of the lines by the earth's magnetic field, the millimeter lines were measured in the following manner. Since O_2 has a magnetic dipole moment, an external magnetic field lifts the $2J + 1$ degeneracy of the different J levels. The earth's magnetic field, although not large enough to produce a resolvable Zeeman multiplet in O_2 , does cause an artificially broadened line shape. In order to eliminate this broadening, an external dc magnetic field was applied to split the Zeeman components further until they were well resolved. At the low dc field values employed

SILICON BOLOMETER DETECTOR

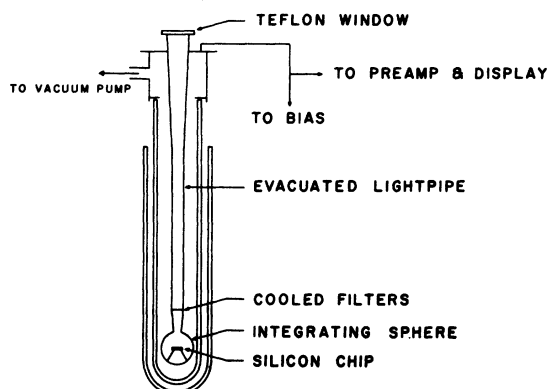


FIG. 3. Diagram of the detector. The silicon-chip detecting element is maintained at a temperature of 1.5 °K.

(12 G or less), the Zeeman pattern is symmetrical about the center frequency. Thus, the companion $\pm M_J$ Zeeman components were measured and averaged to obtain the frequency for the unperturbed zero-field line. The small ac Zeeman modulation field used in the detection was superimposed on the dc field. The resulting Zeeman components of the millimeter wave lines were so strong that they could be displayed and measured on an oscilloscope screen. Unfortunately, the submillimeter wave lines were not sufficiently strong to allow measurement of individual Zeeman components in this manner.

THEORY

The theory of O_2 has been developed and elaborated by many people.^{6, 9-13} When centrifugal-

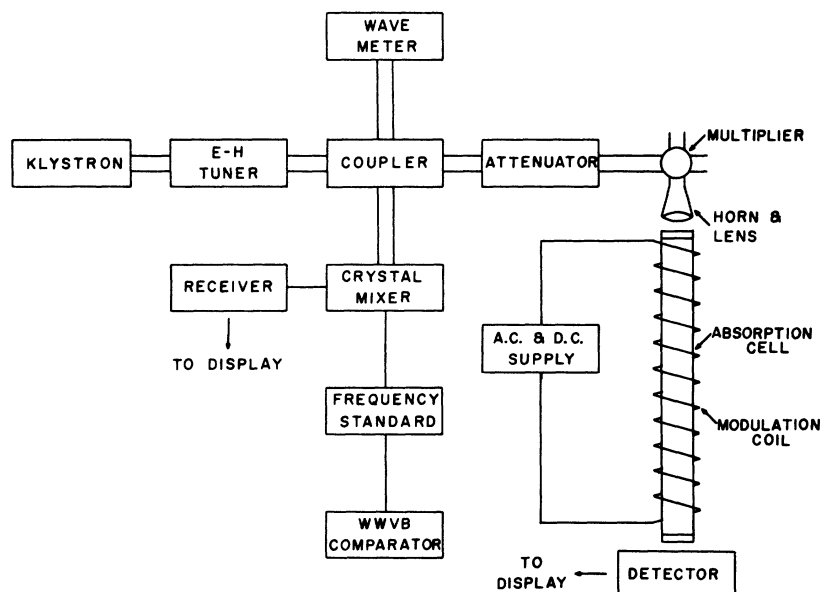


FIG. 2. Block diagram of the Zeeman modulation spectrometer.

distortion effects are neglected, the rotational Hamiltonian¹³ may be expressed in the form

$$\mathcal{H} = B\vec{N}^2 + \mu\vec{N} \cdot \vec{S} + \frac{2}{3}\lambda(3S_z^2 - \vec{S}^2), \quad (1)$$

where the first term on the right-hand side represents the end-over-end rotational energy; the second, the spin-molecular rotational interaction; and the last, the electronic spin-spin interaction assumed to be axially symmetric about the bond axis z .

If centrifugal-distortion effects are considered for the terms in B and μ , the Hamiltonian has the form

$$\begin{aligned} \mathcal{H} = & B_0\vec{N}^2 + B_1\vec{N}^4 + \mu_0\vec{N} \cdot \vec{S} \\ & + \mu_1(\vec{N} \cdot \vec{S})\vec{N}^2 + \frac{2}{3}\lambda(3S_z^2 - \vec{S}^2). \end{aligned} \quad (2)$$

The corresponding corrections for λ are described below in Eqs. (5) and (6).

In the present work, the theory of irreducible tensor operators was found to be a useful technique for evaluation of the matrix elements of the O_2 Hamiltonian. The matrix elements were obtained in a two-step process. The first step requires that the Hamiltonian be written in spherical tensor form. This standard reformulation¹⁴ is

$$\begin{aligned} \mathcal{H} = & B_0(\vec{N}^{(1)} \times \vec{N}^{(1)})^{(0)} \cdot \vec{D}^{(0)} + B_1[(\vec{N}^{(1)} \times \vec{N}^{(1)})^{(0)} \cdot \vec{D}^{(0)}]^2 + \mu_0\vec{N}^{(1)} \cdot \vec{S}^{(1)} + \mu_1(\vec{N}^{(1)} \cdot \vec{S}^{(1)}) \\ & \times [(\vec{N}^{(1)} \times \vec{N}^{(1)})^{(0)} \cdot \vec{D}^{(0)}] + \lambda(\vec{S}^{(1)} \times \vec{S}^{(1)})^{(2)} \cdot \vec{C}^{(2)}, \end{aligned} \quad (3)$$

where $\vec{D}^{(0)}$ is the zeroth-rank spherical tensor form of the cartesian unit tensor; $\vec{C}^{(2)}$ is the second-rank spherical tensor form of the second-rank space-fixed tensor $C_{IJ} = \frac{2}{3}(3\Phi_{Iz}\Phi_{Jz} - \delta_{IJ})$, in which Φ_{Iz} is the direction cosine between the space-fixed I axis and the body-fixed z axis, etc.; and $\vec{N}^{(1)}$ and $\vec{S}^{(1)}$ are the first-rank spherical tensor forms of the operators \vec{N} and \vec{S} , respectively.

With the Hamiltonian in this form [Eq.(3)], one may use the theories of irreducible tensor operators¹⁵ to write the matrix elements

$$\begin{aligned} \langle \phi' | \mathcal{H} | \phi \rangle = & \{B_0N(N+1) + B_1N^2(N+1)^2 + \frac{1}{2}\mu_0[J(J+1) - N(N+1) - S(S+1)] + \frac{1}{2}\mu_1N(N+1) \\ & \times [J(J+1) - N(N+1) - S(S+1)]\} \delta_{J, J'} \delta_{M_J, M_{J'}} \delta_{N, N'} \delta_{S, S'} \\ & + 2\left(\frac{5}{6}\right)^{1/2}\lambda(-1)^{J+N'+S} \begin{Bmatrix} J & N' & S \\ 2 & S & N \end{Bmatrix} (N' \| 3\Phi_{z^2} - 1 \| N) \delta_{J, J'} \delta_{M_J, M_{J'}} \delta_{S, S'}, \end{aligned} \quad (4)$$

where $\vec{J} = \vec{N} + \vec{S}$, \vec{N} is the rotational angular momentum and \vec{S} is the total electron spin. The term $|\phi\rangle$ represents the set of basis vectors diagonal in the quantum numbers J, M_J, N , and S . The reduced matrix element associated with λ , $(N' \| 3\Phi_{z^2} - 1 \| N)$, yields a nonzero value only for matrix elements diagonal or off-diagonal by 2 in the rotational quantum number N . In these two cases, λ may be expanded as shown below¹³:

$$\lambda = \lambda_0 + \lambda_1 N(N+1) \quad \text{for } N = N', \quad (5)$$

$$\lambda = \lambda_0 + \lambda_1(J^2 + J + 1) \quad \text{for } N = J - 1 \text{ and } N' = J + 1. \quad (6)$$

It is clear that the terms associated with B_0 , B_1 , μ_0 , and μ_1 could have been obtained just as easily without this new approach. Considerable work, involving change of basis vectors by means of Clebsch-Gordan coefficients, would, however, have been required for dealing with the λ term. These complications do not arise in the irreducible tensor operator theory since all changes of basis have already been accomplished during the derivation of the various theorems.

The Hamiltonian matrix consists of 3×3 submatrices which may be diagonalized in closed form. The resulting energy levels for the n th triplet are given:

$$\begin{aligned} E(J = n) = & B_0n(n+1) + B_1n^2(n+1)^2 + \frac{2}{3}\lambda_0 + \frac{2}{3}\lambda_1n(n+1) - \mu_0 - \mu_1n(n+1), \\ E(J = n-1) = & B_0(n^2 - n + 1) + B_1(n^4 - 2n^3 + 7n^2 - 6n + 2) - \frac{1}{3}\lambda_0 - \frac{1}{3}\lambda_1(n^2 - n + 4) - \frac{3}{2}\mu_0 - \frac{1}{2}\mu_1(7n^2 - 7n + 4) \\ & + \left\{ [B_0(2n-1) + B_1(4n^3 - 6n^2 + 6n - 2) - \lambda_0(2n-1)^{-1} - \lambda_1(7n^2 - 7n + 4)(6n-3)^{-1} \right. \\ & \left. - \frac{1}{2}\mu_0(2n-1) - \frac{1}{2}\mu_1(2n^3 - 3n^2 + 9n - 4)]^2 + 4[\lambda_0 + \lambda_1(n^2 - n + 1)]^2 n(n-1)(2n-1)^{-2} \right\}^{1/2}, \quad (7) \\ E(J = n+1) = & B_0(n^2 + 3n + 3) + B_1(n^4 + 6n^3 + 19n^2 + 30n + 18) - \frac{1}{3}\lambda_0 - \frac{1}{3}\lambda_1(n^2 + 3n + 6) - \frac{3}{2}\mu_0 - \frac{1}{2}\mu_1(7n^2 + 21n + 18) \\ & - \left\{ [B_0(2n+3) + B_1(4n^3 + 18n^2 + 30n + 18) - \lambda_0(2n+3)^{-1} - \lambda_1(7n^2 + 21n + 18)(6n+9)^{-1} \right. \\ & \left. - \frac{1}{2}\mu_0(2n+3) - \frac{1}{2}\mu_1(2n^3 + 9n^2 + 21n + 18)]^2 + 4[\lambda_0 + \lambda_1(n^2 + 3n + 3)]^2 (n+1)(n+2)(2n+3)^{-2} \right\}^{1/2}. \end{aligned}$$

TABLE I. $^{18}\text{O}_2$ transition frequencies (MHz).

Transition	Observed ^a frequency	Predicted ^a frequency	Deviation
$\nu_+(1)$	57 239.907(20)	57 239.952(12)	-0.045
$\nu_+(3)$	58 899.771(27)	58 899.732(12)	+0.039
$\nu_+(5)$	59 811.414(34)	59 811.404(15)	+0.010
$\nu_+(7)$	60 505.782(62)	60 505.840(47)	-0.058
$\nu_-(3)$	61 529.854(32)	61 529.864(18)	-0.010
$\nu_-(5)$	59 871.473(23)	59 871.464(19)	+0.009
$\nu_-(7)$	58 962.067(24)	58 962.047(15)	+0.020
$\nu_-(9)$	58 270.727(9)	58 270.794(46)	-0.067
$1(2) \rightarrow 3(2)^b$	378 831.51(10)	378 831.51(2)	...

^a All errors quoted are one standard deviation.

^b This line was not excluded from the fit.

These expressions are similar to those given by Welch and Mizushima¹⁶ but contain corrections for several small errors.

EXPERIMENTAL RESULTS AND ANALYSIS OF DATA

The observed millimeter transitions for $^{18}\text{O}_2$ are listed in Table I. The error limits quoted for all numbers are one standard deviation. Figure 4 is a photograph of the $\nu_+(5)$ transition after it had been split into Zeeman components by the external dc magnetic field. The relative heights of the signals do not give a correct measure of the relative intensity of the Zeeman components. The larger signal strength recorded for the outer components results from their greater sensitivity to the modulating field.

The $n(J) = 1(2) \rightarrow 3(2)$ transition of $^{18}\text{O}_2$ is also listed in Table I. Figure 5 shows the chart recorder tracing of this line.

The $n(J) = 1(2) \rightarrow 3(2)$ transition of $^{16}\text{O}_2$ was remeasured. The measured frequency is 424 763.21(10) MHz as compared to the value of 424 763.80(20) MHz previously reported by McKnight and Gordy.⁴ The improved accuracy results from the improved signal-to-noise ratio, about a factor of 10, obtained with the low-temperature silicon



FIG. 4. Zeeman pattern of the $\nu_+(5)$ fine-structure transition in $^{18}\text{O}_2$. The increasing height of the outer components is due to their greater sensitivity to Zeeman modulation.

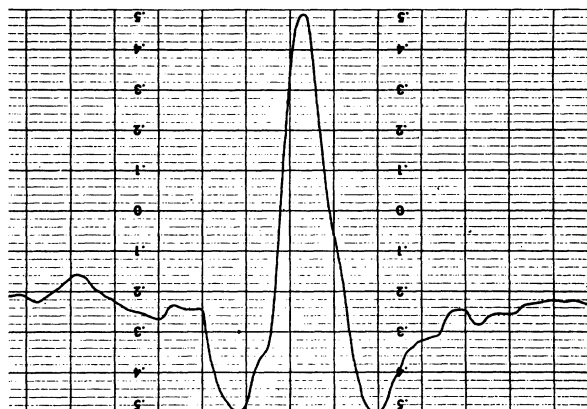


FIG. 5. Second derivative of the absorption contour for the $n(J) = 1(2) \rightarrow 3(2)$ submillimeter rotational transition of $^{18}\text{O}_2$. The measured peak frequency is 378 831.51(20) MHz.

bolometer. The earlier signal, detected with a point-contact diode, was barely above the noise level. The difference of 0.59 MHz in these measurements, we believe, is due mostly to lower precision in the earlier one.

The $^{18}\text{O}_2$ frequencies were analyzed by means of a nonlinear weighted least-squares computer program to obtain the molecular parameters. The third column of Table I lists the frequencies predicted from the least-squares fit, with the predicted transition excluded from the data used in the analysis.

The first column in Table II lists the molecular parameters obtained from the analysis with all nine transition frequencies included in the fitting. The constant B_0 was also calculated from the $^{16}\text{O}_2$ parameter¹⁶ by standard isotopic-substitution techniques.¹⁷ Using the assumption that μ_0 and

TABLE II. Molecular parameters of $^{18}\text{O}_2$.

	Fitted value ^a	Isotopic substitution value ^b
B_0	38 313.721(2) MHz	38 313.155 MHz
B_1	...	-0.115 00 MHz
λ_0	59 496.708(12) MHz	59 501.342 MHz
λ_1	0.0521(3) MHz	0.0585 MHz
μ_0	-224.438(3) MHz	-224.460 MHz
μ_1	-0.000 29(5) MHz	-0.0002 MHz
B_e	38 518.6(6.3) MHz	...
r_e	1.207428(100) Å	...

^a Derived from present measurements on $^{18}\text{O}_2$.

^b Derived from previous $^{16}\text{O}_2$ constants by isotopic substitution techniques. The $^{16}\text{O}_2$ constants used are those from Welch and Mizushima (see Ref. 16): $B_0 = 43 100.518$ MHz, $B_1 = -0.144 962$ MHz; $\lambda_0 = 59 501.342$ MHz, $\lambda_1 = 0.058 47$ MHz, $\mu_0 = -252.586$ MHz, and $\mu_1 = -0.000 246 4$ MHz.

μ_1 vary inversely as the reduced mass and reduced-mass squared, respectively, we were also able to obtain isotopic values for these parameters from the $^{16}\text{O}_2$ constants. Since only one rotational transition was measured for $^{18}\text{O}_2$, it was not possible to obtain the centrifugal stretching parameter B_1 from the data. Instead, B_1 was calculated from the $^{16}\text{O}_2$ value by isotopic substitution techniques and was held fixed during the fitting procedure. The constants λ_0 and λ_1 have no simple isotopic dependence; thus the isotopic values for these constants were set equal to the $^{16}\text{O}_2$ values. These isotopic values are listed in the second column of Table II.

The effective internuclear distance r_0 for the ground vibrational state was obtained from B_0 with the expression

$$r_0 = (h/8\pi^2\mu B_0)^{1/2}, \quad (8)$$

where h is Planck's constant and μ is the reduced mass of the molecule. With $h = 6.62559(16) \times 10^{-27}$ erg sec and the ^{18}O mass = $2.987635(36) \times 10^{-23}$ g,

$$(r_0)_{18,18} = 1.210651(17) \text{ \AA}.$$

The equilibrium values for B_e and r_e were derived in the following manner. Corrections for the ground-state vibration effects were calculated with the first-order expression¹⁷

$$B'_e = B_0 + \frac{1}{2}\alpha, \quad (9)$$

with the α obtained from that for $^{16}\text{O}_2$. The most accurate value of α for $^{16}\text{O}_2$, $\alpha = 0.01593(50) \text{ cm}^{-1} = 477.6(15.0) \text{ MHz}$, is probably that obtained by Albritton *et al.*¹⁸ from an analysis of the complete set of early optical measurements of Babcock and Herzberg.¹⁹ Because a high-speed computer was not available to them, Babcock and

Herzberg derived their constants from only the simpler transitions.

The corresponding value of α for $^{18}\text{O}_2$ may be found with the expression¹⁷

$$\begin{aligned} (\alpha)_{18,18} &= (\mu_{16,16}/\mu_{18,18})^{3/2}(\alpha)_{16,16} \\ &= 400.0(12.6) \text{ MHz}. \end{aligned} \quad (10)$$

Thus $B'_e = 38313.721(2) + \frac{1}{2}(400.0) \text{ MHz} = 38513.8(6.3) \text{ MHz}$. A correction was also made for the rotation of the non-spherically-distributed electron cloud with the relation²⁰

$$B_e = (1 - g_r)B'_e, \quad (11)$$

where g_r is the molecular rotational g factor. The value of g_r for $^{16}\text{O}_2$ was found by Evenson and Mizushima²¹ to be $-1.25(8) \times 10^{-4}$. With the approximation that g_r is the same for $^{18}\text{O}_2$ as for $^{16}\text{O}_2$, we obtain

$$(B_e)_{18,18} = 38518.6(6.3) \text{ MHz}$$

and

$$(r_e)_{18,18} = 1.207428(100) \text{ \AA}.$$

This result compares well with the r_e value²² $1.207428(100)$ for $^{16}\text{O}_2$. The ratio $(r_e)_{16,16}/(r_e)_{18,18}$ is $1.000005(123)$. If the values were strictly correct, this ratio should be exactly unity since the r_e values are presumably not influenced by the isotopic changes. Higher-order corrections,²³ including that due to wobble stretching, which cannot be evaluated from the present data, are neglected.

ACKNOWLEDGMENTS

We would like to thank Dr. Frank DeLucia and Dr. Paul Helminger for valuable assistance.

*Work supported by the National Science Foundation Grant No. GP-34590 and by the U. S. Army Research Office (Durham) Grant No. DA-ARO-D-31-124-72-G96.
¹J. H. Burkhalter, R. S. Anderson, W. V. Smith, and W. Gordy, *Phys. Rev.* **77**, 152 (1950); *Phys. Rev.* **79**, 651 (1950).
²R. W. Zimmerer and M. Mizushima, *Phys. Rev.* **121**, 152 (1961).
³B. G. West and M. Mizushima, *Phys. Rev.* **143**, 31 (1966).
⁴J. S. McKnight and W. Gordy, *Phys. Rev. Lett.* **21**, 1787 (1968).
⁵S. L. Miller, A. Javan, and C. H. Townes, *Phys. Rev.* **82**, 454 (1951).
⁶M. Tinkham and M. W. P. Strandberg, *Phys. Rev.* **97**, 937 (1955).
⁷W. C. King and W. Gordy, *Phys. Rev.* **90**, 319 (1953); *Phys. Rev.* **93**, 407 (1954).

⁸P. Helminger, F. De Lucia, and W. Gordy, *Phys. Rev. Lett.* **25**, 1397 (1970).
⁹H. A. Kramers, *Z. Phys.* **53**, 422 (1929).
¹⁰M. H. Hebb, *Phys. Rev.* **49**, 610 (1936).
¹¹R. Schlapp, *Phys. Rev.* **51**, 342 (1937).
¹²S. L. Miller and C. H. Townes, *Phys. Rev.* **90**, 537 (1953).
¹³M. Mizushima and R. M. Hill, *Phys. Rev.* **93**, 745 (1954).
¹⁴See, for example, R. L. Cook and F. C. De Lucia, *Am. J. Phys.* **39**, 1433 (1971).
¹⁵A. R. Edmonds, *Angular Momentum in Quantum Mechanics* (Princeton U. P., Princeton, N.J. 1960); or Ref. 14.
¹⁶W. M. Welch and M. Mizushima, *Phys. Rev. A* **5**, 2692 (1972).
¹⁷G. Herzberg, *Spectra of Diatomic Molecules* (Van Nostrand, Princeton, N.J., 1950), Sec. III 2.

¹⁸D. L. Albritton, W. J. Harrop, A. L. Schmeltekopf, and R. N. Zare, *J. Mol. Spectry.* 46, 103 (1973). The value of α used for the $^3\Sigma_g^-$ of $^{18}\text{O}_2$ was privately communicated to us by D. L. Albritton.

¹⁹H. D. Babcock and G. Herzberg, *Astrophys. J.* 108, 167 (1948).

²⁰W. Gordy and R. L. Cook, *Microwave Molecular Spectra*

(Interscience, New York, 1970), Sec. 11.7.

²¹K. M. Evenson and M. Mizushima, *Phys. Rev. A* 6, 2197 (1972).

²²J. S. McKnight, Ph.D. thesis (Duke University, (1969). (unpublished).

²³See Ref. 19, Sec. 13.6b.